Bioorganic & Medicinal Chemistry 21 (2013) 540–546

Contents lists available at SciVerse ScienceDirect

Bioorganic & Medicinal Chemistry

journal homepage: www.elsevier.com/locate/bmc

Molecular docking and synthesis of novel quinazoline analogues as inhibitors of transcription factors NF-κB activation and their anti-cancer activities

Lu Xu, Wade A. Russu *

Department of Pharmaceutics and Medicinal Chemistry, Thomas J. Long School of Pharmacy and Health Sciences, University of the Pacific, Stockton, CA 95211, USA

ARTICLE INFO

Article history:
Received 24 August 2012
Revised 20 October 2012
Accepted 30 October 2012
Available online 15 November 2012

Keywords:
Quinazoline
NF-κB cancer
Apoptosis

ABSTRACT

NF-kB is a transcription factor protein complex that can be found in almost all animal cell types and is a key player in some cancers and inflammatory responses. It can enhance the proliferation rate, reduce apoptosis, as well as creating more blood flow to ensure the survival of cancer, thus blocking the NF-kB pathway has potential therapeutic benefit. We designed a series of compounds based on a quinazoline scaffold pharmacophore model which may have high binding affinity with the p50 subunit of NF-kB. The compound series with phenyl substitution at the 2 position of the quinazoline proved to be more effective at inhibiting NF-kB function both theoretically and experimentally. These compounds also reduce the proliferation of numerous tumor cell lines and the mean GI_{50} for compound **2a** is 2.88 μM against the NCI-60 cell line. At the same time, compound **2a** can induce significant apoptosis in EKVX cell line at the concentration of 1 μM.

1. Introduction

The constitutive activation of nuclear kappa B (NF-κB) family of transcription factors has been implicated in various disease states including inflammation and cancer.[1] The relevance of this transcriptional activity to cancer is thought to be linked to the transcription control of key antiapoptotic genes that encode B-cell lymphoma-2 (Bcl-2) and inhibitor of apoptosis (IAP) family proteins.[2] Over expression of these antiapoptotic genes can prevent tumor cells from undergoing programmed cell death. These effects in turn contribute to processes of tumorigenesis and resistance to therapies.[3]

The NF-κB proteins consist of five family members. These five proteins, named Rel (c-Rel), RelA (p65), RelB, NF-κB1 (p50), and NF-κB2 (p52), share a common domain called a Rel homology domain (RHD) and form active transcription factors through homo[4] and hetero-dimerization[5] capable of binding DNA at specific promoter sequences. The p50 and p52 proteins come from larger proteins, p105 and p100 respectively, through post translational processes. Control of NF-κB transcriptional activation is the result of signal transduction pathway activation. For example, one well studied signaling pathway that activates NF-κB controlled gene transcription is the tumor necrosis factor (TNF) pathway.[6] Inactive dimers of NF-κB are held in complex with inhibitors of κB (IκB) in the cytosol of unstimulated cells.[7] Upon stimulation with TNF the TNF receptor (TNFR) initiates a phosphorylation cascade that results in inhibitor of κB kinase (IKK) phosphorylation of and subsequent proteosomal degradation of IκB, and the release and translocation of transcriptionally active NF-κB to the cell nucleus.[6] What gene sets are actively transcribed depends on which NF-κB dimer form is active. There are several strategies for inhibiting NF-κB activity.

The activity of NF-κB may be inhibited directly or indirectly. Direct strategies involve inhibitors that interact with one or more of the NF-κB family proteins to prevent their function. These inhibitors may prevent dimerization of NF-κB family members or prevent DNA binding. Indirect strategies involve inhibitors of molecules that affect NF-κB function. Inhibitors that target molecules upstream of NF-κB such as IKK, cytokines and cytokine receptors or prevent NF-κB degradation, such as proteasome inhibitors have been investigated.[8]

The NF-κB inhibitors that are predicted to interact directly with p50 to prevent DNA binding include the triazine, coumarin, and quinazoline chemical classes, among others.[9–11] Extensive docking studies have been performed on some of these in order to identify important elements for binding and pharmacophore development.[12] Here we report our efforts toward the discovery of new inhibitors of the NF-κB controlled transcriptional pathway by making use of previously reported pharmacophore models and lead molecules based on a quinazoline scaffold.

2. Results and discussion

2.1. Design and molecular docking

We designed a series of potential inhibitors of NF-κB transcriptional activation based upon a reported pharmacophore model for

* Corresponding author.
E-mail address: wrussu@pacific.edu (W.A. Russu).

0968-0896/$ - see front matter © 2012 Elsevier Ltd. All rights reserved.
http://dx.doi.org/10.1016/j.bmc.2012.10.051

Table 1
Calculated binding energies of compounds docked to p50. Energies were calculated using AutoDock 4.2

Compound	ΔG (kcal/mol)
1a	−9.09
1b	−7.63
2a	−9.78
2b	−7.81
3a	−8.41
3b	−6.27
4a	−8.86
4b	−6.89
5a	−9.09
5b	−8.22
6a	−8.52
6b	−6.98

binding p50, derived from a series of 6-aminoquinazoline analogs.[13] Upon examining the proposed binding mode of one of these analogs to p50 we discovered the possibility that substitution at the 2-position of the quinazoline ring may be tolerated and result in a gain of binding affinity. We also reasoned, based on the binding hypothesis, that the 6-amino group may not be necessary for binding to the target. A series of 2-phenylquinazolines linked from the 4-position via aminoethyl or piperazinyl group to an aromatic substituent were designed. A second series without a 2-phenyl substituent were also designed for comparison. A total of 22 molecules were designed based upon readily available starting materials, a previously report pharmacophore model and were docked to the NF-kB p50 protein (Autodock 4.2). The molecules were synthesized and evaluated for their inhibitory effect against the HepG2 cell line at 1 μM. A two-tailed Pearson correlation was performed which revealed a relationship between inhibition and docking free energy (see Supplementary data Fig. 1). Representative examples displaying low, medium and high binding free energies were chosen for further study (Table 1). Figure 1 depicts the hypothesis for binding to the p50 protein of **2a** and **2b**. Docking results are reported in Table 1.

Examination of Table 1 reveals that for every selected pair the 2-phenyl analog is predicted to bind with a more negative free energy and thus a stronger association with the p50 protein. In each case, the predicted binding geometry of the lowest energy docked complex placed the 2-phenyl substituent in a hydrophobic pocket where favorable intermolecular interactions with the aromatic side chain of Phe53 and other hydrophobic amino acids contribute to binding. Figure 1 depicts the predicted geometry of **2a** compared to **2b** bound to the p50 protein. Other notable intermolecular interactions include the **2a** indole ring system with His64 through pi–pi stacking and with the Val58 backbone amide through an H-bond.

2.2. Synthesis of quinazoline analogues

The designed molecules were synthesized in few steps starting from either 4-chloroquinazoline or 2-phenyl-4-chloroquinazoline. The quinazoline starting materials were either allowed to react with the appropriate amine to give the final molecule directly or with mono-Boc piperazine followed by removal of the Boc group and subsequent reductive amination with an aldehyde in order to provide the final molecule. Molecules **1–6 a** and **b** series analogs were synthesized according to Scheme 1. Yields of final recrystallized products for the one or three step synthetic procedure were moderate to good.

2.3. TNFα enhances anti-proliferation effects of designed molecules

The HepG2 cell line was used to assess whether the paired molecular series antitumor cell effects correlate with NF-κB

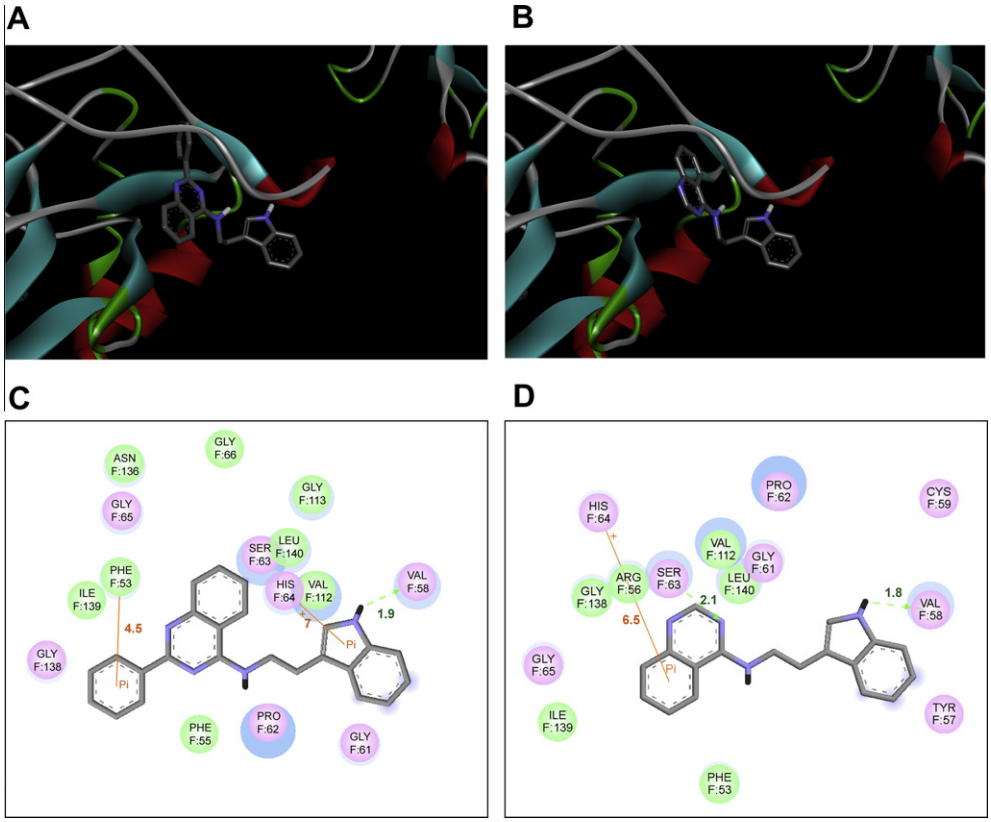

Figure 1. Representations of lowest energy docking poses of compounds **2a** (panel A) and **2b** (panel B) bound to the NF-κB p50 protein. Intermolecular interactions between p50 and **2a** (panel C) and **2b** (panel D) are highlighted by 2-D interaction maps.

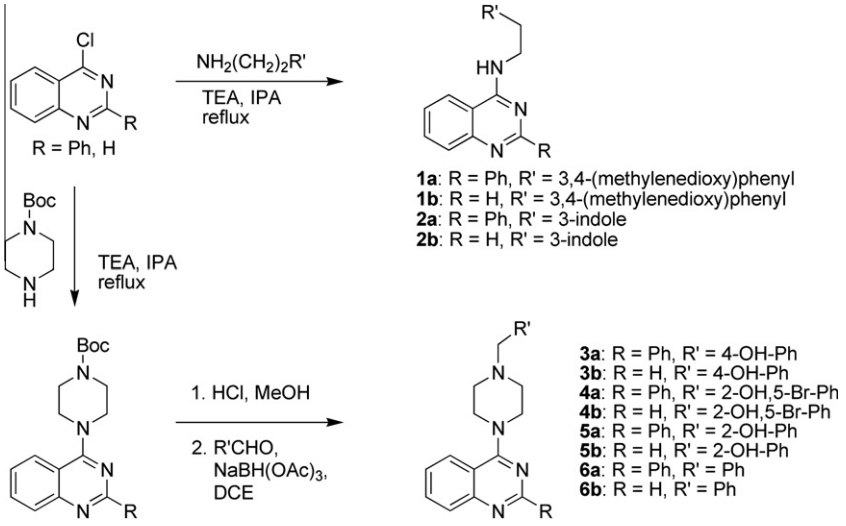

Scheme 1. Chemical synthesis of molecules **1–6**.

signaling. When stimulated with tumor necrosis factor (TNFα) the HepG2 cell line activates both pro and anti-apoptosis genes.[14] These anti-apoptosis genes are expressed in an NF-κB dependent manner. Therefore, HepG2 cell growth will be inhibited to a greater extent when treated with an NF-κB pathway inhibitor in the presence of TNFα, than in the absence of TNFα, by increased apoptosis due to shifting the balance between pro and anti-apoptosis proteins toward pro-apoptosis. Table 2 reports the percent growth of HepG2 cells treated with 50 μM of molecules **1–6** in the presence or absence of TNFα. For molecules **1–3** it is evident that they are more effective in the presence of TNFα (p <0.05), and that the growth inhibitory effect is of a greater magnitude for the 2-phenyl substituted analogs. This result supports the hypothesis that the 2-phenyl substituted analogs are better NF-κB pathway inhibitors. For molecules **4–6** the results varied. For example, **4b** was more effective in the presence of TNFα whereas **4a** was not. Neither of molecule **5a** or **5b** showed a significant difference in the presence of TNFα (p >0.4). Molecule **6a** was better at inhibiting the growth of HepG2 cells in the presence of TNFα whereas **6b** did not show a significant difference (p >0.4). Molecules **1–3** and **6** behaved as expected in that the 2-phenyl analogs were better at inhibiting cell growth in the presence of TNFα than in the absence of TNFα. Only molecule **4** showed the opposite tendency.

Table 2
Percent cell growth of HepG2 cells treated with compounds **1–6**[a] in the absence and presence of TNFα

Compound	% Cell growth (±SD)[b]	
	without TNFα	With TNFα
1a	−30.7 (2.7)	−46.8 (7.0)
1b	−20.1 (1. 7)	−28.1 (2.3)
2a	−35.3 (2.3)	−46.7 (6.4)
2b	−22.3 (2.9)	−30.0 (3.0)
3a	−37.6 (2.6)	−49.1 (6.1)
3b	−5.3 (1.4)	−13.3 (6.6)
4a	15.5 (3.1)	13.0 (2.4)
4b	−22.0 (2.5)	−29.9 (2.4)
5a	14.6 (1.2)	13.0 (2.4)
5b	−21.7 (5.9)	−26.0 (5.7)
6a	30.7 (0.4)	13.7 (1.2)
6b	−16.7 (4.5)	−17.6 (4.8)

[a] 50 μM.
[b] SD: standard deviation for 3 independent experiments.

2.4. Designed molecules downregulate NF-κB dependent gene transcription

We next turned our attention to assessing whether the new compounds could inhibit NF-κB dependent gene transcription. For this inquiry we used a Luciferase reporter assay. HepG2 cells were transfected with the Luciferase gene under control of an NF-κB promoter.[15] The molecules from both the 2-phenyl and 2-H series were assayed in addition to a commercially available quinazoline-based NF-κB inhibitor called QNZ.[11,16] The results of the Luciferase reporter assay are summarized in Figure 2. The results of the Luciferase reporter assay mirror the HepG2 growth inhibition experiment in that **1a**–**3a** and **6a** significantly decrease (p <0.05) NF-κB dependent Luciferase expression in the presence of TNFα, whereas **1b**–**3b** and **6b** did so to a lesser extent. There does not appear to be a significant difference in the ability of **4a** and **5a**, to inhibit the NF-κB Luciferase expression, compared to their 2-H analogs **4b** and **5b** (p = 0.8 and 0.1 respectively) which is also consistent with the aforementioned growth inhibition experiment, and suggests that these molecules may exert their antitumor activity by a different or multiple mechanisms. Also shown in Figure 2 is the effect of **2a** on NF-κB dependent Luciferase expression at different doses compared to the commercially available NF-κB pathway inhibitor QNZ. The molecules **2a** and QNZ have similar activity.

2.5. Designed molecule induce apoptosis in tumor cells

Encouraged by the growth inhibition of human tumor cell lines by the new designed molecules and their ability to inhibit NF-κB transcriptional activity, we next assessed whether these activities were accompanied by apoptosis. We compared the relative amount of apoptosis of EKVX cells treated with TNFα in the absence of and presence of **2a** using terminal deoxynucleotidyltransferase (TdT) nick-end labeling (TUNEL) assay. The TNFα stimulated cells did not show apoptosis when stained with TUNEL reagent in the absence of **2a**. However, TNFα treated cells in the presence of **2a** showed an increase in the number of TNNEL positive cells when examined under fluorescence microscopy. This is a positive indication that **2a** can initiate apoptosis in the presence of TNFα, which together with the cell growth inhibition experiments and NF-κB dependent Luciferase expression strongly suggests that molecule **2a** exerts its antitumor cell activity by inhibition of NF-κB. Figure 3 depicts the TUNEL assay results.

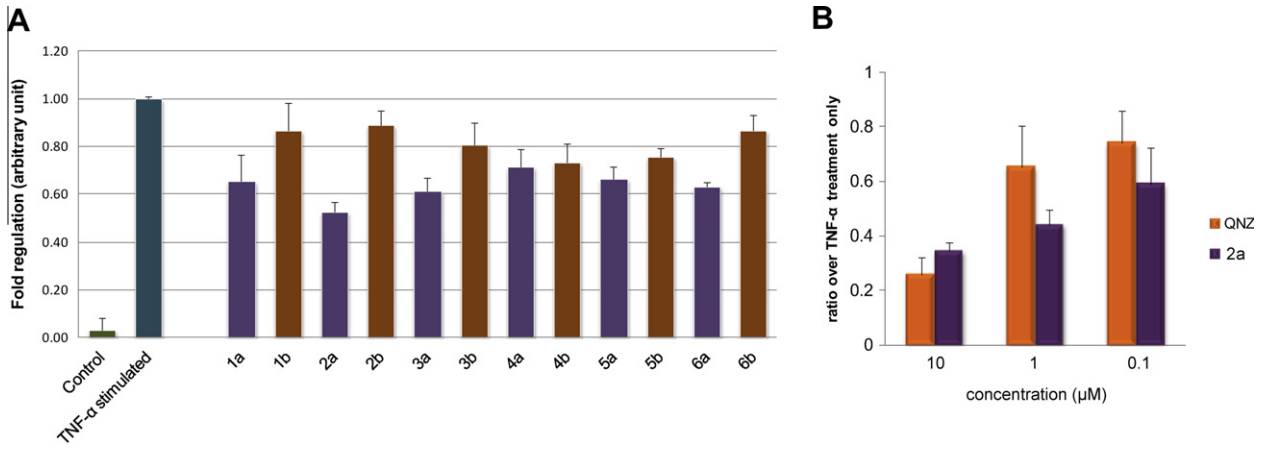

Figure 2. Luciferase reporter assay performed with transfected HepG2 cells pretreated with 1 μM of indicated molecules **1**–**6** and stimulated with TNFα. (A) Bars represent relative NF-κB dependent luciferase activity compared to TNFα stimulated cells in the absence of molecules **1**–**6**. Control represents luciferase activity in non-TNFα stimulated HepG2 cells in the absence of experimental molecules; (B) Comparison of NF-κB dependent luciferase activity in TNFα stimulated HepG2 cells pre-treated with either QNZ or **2a**.

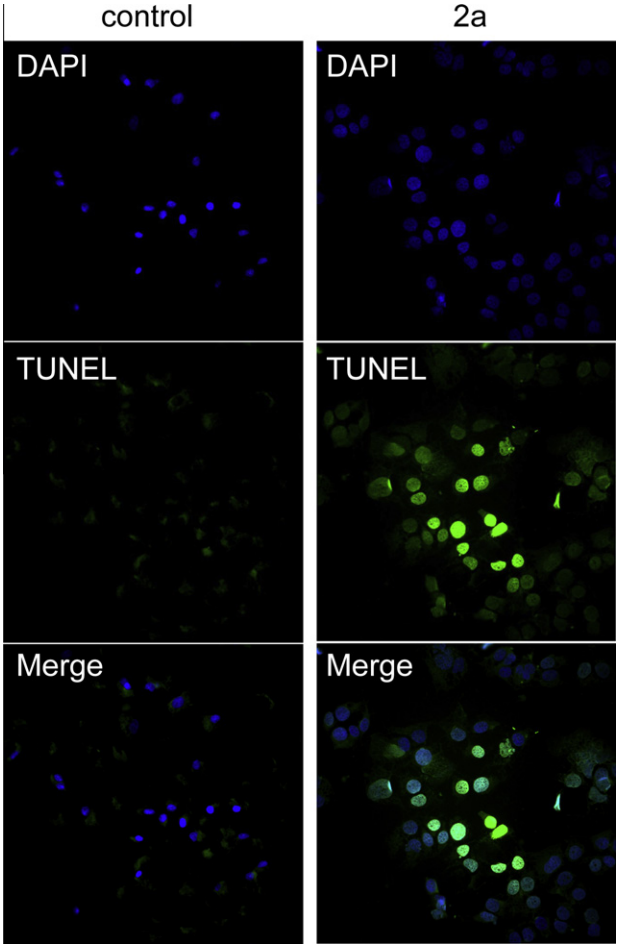

Figure 3. EKVX cells in the absence (control) of or pretreated with **2a** (1 μM) were stimulated with TNFα (20 ng/mL) for 18 h and then subjected to TUNEL assay.

2.6. NCI-60 cell line activity

In order to test the designed molecules ability to inhibit the growth of a variety of tumor cells, these molecules were screened against the National Cancer Institute's 60 tumor cell line panel (NCI-60) within the context of the Developmental Therapeutics Program.[17] Molecules **2a** and **2b** were selected for dose response testing and fifty percent growth inhibition concentrations (GI_{50}) were determined according to the SRB protocol.[18] Table 3 gives a comparison of GI_{50} values for both **2a** and **2b** on all cell lines tested. In all cases but two, molecule **2a**, the 2-phenyl substituted analog, is more effective at inhibiting the growth of tumor cells.

Table 3
NCI dose response report of **2a** and **2b**

Tissue type	Cell line	GI_{50} (μM)		Tissue type	Cell line	GI_{50} (μM)	
		2a	**2b**			**2a**	**2b**
Colon cancer	COLO 205	2.2	28.2	Ovarian cancer	IGROV1	3.2	14.1
	HCC-2998	2.1	26.3		OVCAR-3	2.9	19.1
	HCT-116	2.8	6.3		OVCAR-4	3.6	1.5
	HCT-15	2.5	24.0		OVCAR-8	2.2	5.5
	KM12	2.8	19.1		NCI/ADR-RES	2.6	5.6
	SW-620	3.0	41.7		SK-OC-3	3.7	58.9
CNS cancer	SF-268	4.6	34.7	Renal cancer	786-0	2.5	33.9
	SF-295	2.0	3.5		A498	2.0	2.8
	SF-539	2.0	39.8		CAKI-1	3.1	2.2
	SNB-19	5.1	50.1		RXF 393	1.9	30.9
	SNB-75	5.9	22.9		SN12C	3.9	30.2
	U251	3.2	30.9		TK-10	2.8	20.4
Melanoma	LOX IMVI	2.2	15.5	Breast cancer	MCF-7	4.2	11.2
	MALME-3 M	2.8	29.5		MDA-MB-231/ATCC	3.1	21.9
	M14	2.6	24.6		HS 578T	3.4	60.3
	MDA-MB-435	2.3	10.2		BT-549	4.4	12.3
	SK-MEL-2	3.0	30.9		T-47D	2.4	12.0
	SK-MEL-28	6.2	25.1		UO-31	3.0	14.5
	UACC-357	3.2	9.8	Prostate cancer	PC-3	2.4	19.5
	UACC-62	2.0	14.1		DU-145	4.7	27.5

3. Conclusion

We have described the design, synthesis and evaluation of quinazoline based NF-κB pathway inhibitors. Based on a previously

reported pharmacophore model, we incorporated a 2-phenyl substitution of the quinazoline ring that enhanced the inhibition of NF-κB dependent gene transcription and initiated apoptosis as assessed by Luciferase and TUNEL assays respectively. While these compounds were designed upon and our results support a NF-κB p50 binding hypothesis, other possible mechanisms such as inhibition of upstream kinases cannot be ruled out at this time. We are currently engaged in a more detailed mechanistic investigation of **2a** and will report our findings in due course.

4. Experimental

4.1. General

All the chemicals were obtained from Sigma–Aldrich and ARCOS, and were used for synthesis without further purification. Proton and ^{13}C NMR were measured by JEOL ECA 600 MHz instrument. Mass spectra were analyzed by KRATOS/ SHIMADZU AXIMA-CFR MALDI-TOF. The luciferase activities were measured using GloMax 96 Microplate Luminometer with Dual injectors (Promega, Medison, WI).

4.2. Synthetic procedures

4.2.1. Synthesis of *N*-(2-(benzo[*d*][1,3]dioxol-5-yl)ethyl)-2-phenylquinazolin-4-amine (1a)

Triethylamine (0.28 ml, 2 mmol) was added to a suspension of 4-chloro-2-phenylquinazoline (0.36 g, 1.5 mmol) and 3,4-methylenedioxyphenethylamine hydrochloride (0.30 g, 1.5 mmol) in 10 ml 2-propanol. The reaction was heated at reflux and monitored using TLC. Once the reaction was finished, solvent was removed under reduced pressure and the residue was purified using column chromatography (3:1 Hexane/Ethyl acetate) to give an off-white solid. (210.5 mg, 38.3% yield): mp 105 °C; ^1H NMR ($CDCl_3$) δ 8.60–8.57 (m, 2H), 7.92 (d, J = 7.92 Hz, 1H), 7.71 (ddd, J = 1.38 Hz, J = 7.08 Hz, 1H), 7.54–7.58 (m, 1H), 7.52–7.345 (m, 3H), 7.38 (ddd, J = 1.20 Hz, J = 7.08 Hz, J = 8.28 Hz, 1H), 6.78 (t, J = 1.68 Hz, 1H), 6.77 (s, 1H), 6.72 (dd, J = 1.56 Hz, 1H), 5.94 (s, 2H), 5.75 (t, J = 4.68 Hz 1H), 4.00 (q, J = 6.90 Hz, 2H), 3.00 (t, J = 6.90 Hz 2H); ^{13}C NMR ($CDCl_3$) δ 160.5, 159.4, 150.5, 147.9, 146.3, 138.9, 132.8, 132.5, 130.0 128.8, 128.4, 128.3, 125.4, 121.7, 120.3, 113.7, 109.1, 108.4, 100.9, 42.4, 35.1; MS Calcd for $C_{23}H_{19}N_3O_2$ 369.1477. Found MS (DART-TOF) m/z 369.1527 $(M+H)^+$.

4.2.2. Synthesis of *N*-(2-(benzo[*d*][1,3]dioxol-5-yl)ethyl)quinazolin-4-amine (1b)

The title compound was prepared starting from 4-chloroquinazoline and 3,4-methylenedioxyphenethylamine hydrochloride using the same procedure described for **1a** to afford a white solid (31.2% yield): mp 187 °C; ^1H NMR ($CDCl_3$) δ 8.66 (s, 1H), 7.80 (d, J = 7.74 Hz, 1H), 7.70 (ddd, J = 1.38 Hz, J = 7.02 Hz, J = 8.40 Hz, 1H), 7.55 (d, J = 1.56 Hz, 1H), 7.41 (ddd, J = 1.20 Hz, J = 7.02 Hz, J = 8.10 Hz, 1H), 6.75 (d, J = 7.86 Hz, 1H), 6.73 (d, J = 1.74 Hz, 1H), 6.67 (dd, J = 1.68 Hz, J = 7.92 Hz, 1H), 5.93 (s, 2H), 5.84 (s, 1H), 3.87 (q, J = 6.84 Hz, 2H), 2.94 (t, J = 6.90 Hz, 2H); ^{13}C NMR ($CDCl_3$) δ 159.4, 155.5, 149.5, 148.1, 146.4, 132.6, 128.7, 126.1, 121.8, 120.4, 115.0, 109.2, 108.6, 101.1, 42.5, 35.0; MS Calcd for $C_{17}H_{15}N_3O_2$ 293.1164. Found MS (DART-TOF) m/z 293.6 $(M+H)^+$.

4.2.3. *N*-(2-(benzo[*d*][1,3]dioxol-5-yl)ethyl)quinazolin-4-amine (2a)

The title compound was prepared starting from 4-chloroquinazoline and 2-(1H-indol-3-yl)ethanamine using the same procedure described for **1a** to afford a white solid (26.6% yield): mp 166 °C; ^1H NMR ($CDCl_3$) δ 8.64–8.58 (m, 2H), 8.19 (s, 1H), 7.91 (dd, J = 0.48 Hz, J = 8.22 Hz, 1H), 7.72–7.66 (m, 2H), 7.52–7.44 (m, 4H), 7.38 (d, J = 8.1 Hz, 1H), 7.32 (ddd, J = 1.20 Hz, J = 7.08 Hz, J = 8.28 Hz 1H), 7.23 (ddd, J = 1.02 Hz, J = 7.08 Hz, J = 8.10 Hz, 1H), 7.14 (ddd, J = 0.90 Hz, J = 7.08 Hz, J = 7.92 Hz, 1H), 7.06 (d, J = 2.20 Hz, 1H), 5.84 (t, J = 5.46 Hz, 1H), 4.12 (q, J = 6.72 Hz 2H), 3.25 (t, J = 7.08 Hz, 2H); ^{13}C NMR ($CDCl_3$) δ 160.8, 159.6, 150.6, 139.2, 136.5, 132.5, 130.2, 128.8, 127.5, 125.4, 122.4, 120.6, 119.7, 118.9, 113.8, 113.3, 111.5, 41.6, 25.1; MS Calcd for $C_{17}H_{15}N_3O_2$ 364.1688. Found MS (DART-TOF) m/z 364.1789 $(M+H)^+$.

4.2.4. *N*-(2-(1*H*-indol-3-yl)ethyl)quinazolin-4-amine (2b)

The title compound was prepared starting from 4-chloroquinazoline and 2-(1H-indol-3-yl)ethanamine using the same procedure described for **1a** to afford a pale yellow solid (52.7% yield): mp 162 °C; ^1H NMR ($CDCl_3$) δ 8.69 (s, 1H), 8.19 (s, 1H), 7.81 (d, J = 7.74 Hz, 1H), 7.69 (ddd, J = 1.38 Hz, J = 7.08 Hz, 8.46 Hz, 1H), 7.66 (dd, J = 1.02 Hz, J = 7.92 Hz, 1H), 7.43 (dd, J = 1.20 Hz, J = 8.22 Hz, 1H), 7.40 (dt, J = 0.90 Hz, J = 8.28 Hz, 1H), 7.36 (ddd, J = 1.20 Hz, J = 7.02 Hz, J = 8.22 Hz, 1H), 7.23 (ddd, J = 1.02 Hz, J = 7.26 Hz, J = 8.28 Hz,1H), 7.14 (ddd, J = 1.02 Hz, J = 7.14 Hz, J = 8.10 Hz, 1H), 7.09 (d, J = 2.4 Hz, 1H), 5.84 (s, 1H), 4.00 (q, J = 6.54 Hz 2H), 3.20 (td, J = 0.54 Hz, J = 6.54 Hz, 2H); ^{13}C NMR ($CDCl_3$) δ 159.3, 155.5, 149.4, 136.6, 132.6, 128.6, 127.5, 125.9, 122.5, 122.3, 120.5, 119.8, 118.8, 115.1, 113.1, 111.5, 41.5, 24.9; MS Calcd for $C_{18}H_{16}N_4$ 288.1375. Found MS (MALDI-TOF) m/z 289.1457 $(M+H)^+$.

4.2.5. Synthesis of 2-phenyl-4-(piperazin-1-yl)quinazoline

Potassium carbonate (1.38 g, 10 mmol) was added to a suspension of 4-chloro-2-phenylquinazoline (1.2 g, 5 mmol) and 1-Boc-piperazine (0.93 g, 5 mmol) in 7 ml DMF. The reaction was heated while refluxing and monitored using TLC. Once finished, the reaction was acidified with acetic acid and a white precipitate formed. The product was filtered and partitioned (CH_2Cl_2: water 1:1). The organic layer was concentrated under pressure and white solid was formed. The white solid was added to 50 ml methanolic HCl and stirred for 1 h followed by the neutralization with $NaHCO_3$. The precipitate (white solid, 1.18 g, 81.4% yield) was filtered and used in the next step without further purification. ^1H NMR ($CDCl_3$) δ 8.56–8.53 (m, 2H), 7.96 (dd, J = 0.66 Hz, J = 8.40 Hz, 1H), 7.88 (dd, J = 0.90 Hz, J = 8.28 Hz, 1H), 7.71 (ddd, J = 1.38 Hz, J = 6.90 Hz, J = 8.40 Hz, 1H), 7.50–7.43 (m, 3H), 7.40 (ddd, J = 1.20 Hz, J = 6.90 Hz, J = 8.28 Hz, 1H), 3.83 (t, J = 4.80 Hz, 4H), 3.13 (t, J = 4.80 Hz, 4H); MS Calcd for $C_{18}H_{18}N_4$ 290.15. Found MS (MALDI-TOF) m/z 290.8 $(M+H)^+$.

4.2.6. Synthesis of 4-((4-(2-phenylquinazolin-4-yl)piperazin-1-yl)methyl)phenol (3a)

2-phenyl-4-(piperazin-1-yl)quinazoline (0.29 g, 1 mmol) and 4-hydroxybenzaldehyde (0.12 g, 1 mmol) dissolved in 10 ml 1,2-dichloroethene and $NaBH(OAc)_3$ (0.21 g, 1.3 mmol) was added. The reaction was stirred at room temperature overnight and then partitioned between saturated aqueous $NaHCO_3$ and ethyl acetate. The organic layer was concentrated under reduced pressure and then purified using column chromatography (6:1 Hexane/Ethyl acetate) to give pale yellow solid. (0.132 g, 33.3% yield): ^1H NMR (DMSO-d_6) δ 9.27 (s, 1H), 8.46–8.43 (m, 2H), 7.96 (dd, J = 0.66 Hz, J = 8.22 Hz, 1H), 7.84 (dd, J = 0.84 Hz, J = 8.22 Hz, 1H), 7.77 (ddd, J = 1.38 Hz, J = 6.90 Hz, J = 8.28 Hz, 1H), 7.47 (m, 4H), 7.10 (dt, J = 2.58 Hz, J = 8.58 Hz, 2H), 6.69 (dt J = 2.76 Hz, J = 9.30 Hz, 2H), 3.78 (t, J = 4.14 Hz, 4H), 3.41 (s, 2H), 2.55 (t, J = 4.62 Hz, 4H); MS Calcd for $C_{25}H_{24}N_4O$ 396.1950. Found MS (MALDI-TOF) m/z 396.7 $(M+H)^+$.

4.2.7. Synthesis of 4-((4-(quinazolin-4-yl)piperazin-1-yl)methyl) phenol (3b)

The title compound was prepared starting from 4-(piperazin-1-yl)quinazoline and 4-hydroxybenzaldehyde using the same procedure described for **3a** to afford white solid (44.7% yield). Mp 188–189 °C; ^{1}H NMR ($CDCl_3$) δ 8.69 (s, 1H), 7.89 (d, J = 8.46 Hz, 1H), 7.86 (dd, J = 0.90 Hz, J = 8.46 Hz, 1H), 7.71 (ddd, J = 1.20 Hz, J = 6.84 Hz, J = 8.22 Hz, 1H), 7.42 (ddd, J = 1.20 Hz, J = 7.08 Hz, J = 8.28 Hz, 1H), 7.15 (d, J = 8.46 Hz, 2H), 6.79 (d, J = 8.46 Hz, 2H), 3.83 (t, J = 4.86 Hz, 4H), 3.52 (s, 2H), 2.64 (t, J = 4.80 Hz, 4H); MS Calcd for $C_{19}H_{20}N_4O$ 320.1637. Found MS (DART-TOF) m/z 321.1715 $(M+H)^+$.

4.2.8. Synthesis of 4-bromo-2-((4-(2-phenylquinazolin-4-yl) piperazin-1-yl)methyl)phenol (4a)

The title compound was prepared starting from 2-phenyl-4-(piperazin-1-yl)quinazoline and 5-bromo-2-hydroxybenzaldehyde using the same procedure described for **3a** to afford white solid (36.8% yield). Mp 189–190 °C; ^{1}H NMR ($CDCl_3$) δ 8.54 (d, J = 1.56 Hz, 1H), 8.53 (s, 1H), 7.99 (d, J = 8.40 Hz, 1H), 7.87 (d, J = 8.22 Hz, 1H), 7.74 (t, J = 7.86 Hz, 1H), 7.51–7.41 (m, 4H), 7.29 (dd, J = 2.40 Hz, 1H), 7.13 (d, J = 2.22 Hz, 1H), 6.75 (d, J = 8.58 Hz, 1H), 5.29 (s, 1H), 3.93 (s, 4H), 3.77 (s, 2H), 2.81 (s, 4H); MS Calcd for $C_{25}H_{23}BrN_4O$ 474.1055. Found MS (DART-TOF) m/z 475.1095 $(M+H)^+$.

4.2.9. Synthesis of 4-bromo-2-((4-(quinazolin-4-yl)piperazin-1-yl)methyl)phenol (4b)

The title compound was prepared starting from 4-(piperazin-1-yl)quinazoline and 5-bromo-2-hydroxybenzaldehyde using the same procedure described for **3a** to afford white solid (37.3% yield): mp 176–178 °C; ^{1}H NMR ($CDCl_3$) δ 8.74 (s, 1H), 7.91 (dd, J = 0.46 Hz, J = 8.40 Hz, 1H), 7.84 (dd, J = 0.84 Hz, J = 8.40 Hz, 1H), 7.74 (ddd, J = 1.38 Hz, J = 6.90 Hz, J = 8.28 Hz, 1H), 7.45 (ddd, J = 1.38 Hz, J = 7.02 Hz, J = 8.28 Hz, 1H), 7.27 (dd, J = 2.58 Hz, J = 8.58 Hz, 1H), 7.11 (d, J = 2.40 Hz, 1H), 6.73 (d, J = 8.64 Hz, 1H), 3.82 (s, 4H), 3.74 (s, 2H), 2.75 (s, 4H); ^{13}C NMR ($CDCl_3$) δ 164.6, 156.8, 154.1, 151.9, 132.8, 131.9, 131.4, 128.9, 125.8, 118.2, 116.7, 111.2, 61.1, 52.5, 49.6; MS Calcd for $C_{19}H_{19}BrN_4O$ 398.0742. Found MS (DART-TOF) m/z 399.0788 $(M+H)^+$.

4.2.10. Synthesis of 2-((4-(2-phenylquinazolin-4-yl)piperazin-1-yl)methyl)phenol (5a)

The title compound was prepared starting from 2-phenyl-4-(piperazin-1-yl)quinazoline and 2-hydroxybenzaldehyde using the same procedure described for **3a** to afford white solid (33.2% yield): mp 171–172 °C; ^{1}H NMR ($CDCl_3$) δ 8.56–8.53 (m, 2H), 7.99 (dd, J = 0.66, J = 8.46 Hz, 1H), 7.86 (dd, J = 0.90 Hz, J = 8.28 Hz, 1H), 7.73 (ddd, J = 1.38 Hz, J = 6.90 Hz, J = 8.46 Hz, 1H), 7.51–7.45 (m, 3H), 7.42 (ddd, J = 1.20 Hz, J = 6.90 Hz, J = 8.28 Hz, 1H), 7.21 (td, J = 1.74 Hz, J = 7.92 Hz, 1H), 7.01 (dd, J = 1.20 Hz, J = 7.38 Hz, 1H), 6.87 (dd, J = 1.20 Hz, J = 8.10 Hz, 1H), 6.81 (td, J = 1.20 Hz, J = 7.38 Hz, 1H), 3.92 (s, 4H), 3.80 (s, 2H), 2.80 (s, 4H); ^{13}C NMR ($CDCl_3$) δ 164.8, 159.4, 157.5, 152.8, 138.4, 132.6, 130.3, 129.2, 129.1, 128.8, 128.4, 125.1, 124.6, 120.7, 119.4, 116.2, 115.4, 61.6, 52.4, 49.7; MS Calcd for $C_{25}H_{24}N_4O$ 396.1950. Found MS (DART-TOF) m/z 396.2042 $(M+H)^+$.

4.2.11. Synthesis of 2-((4-(quinazolin-4-yl)piperazin-1-yl) methyl)phenol (5b)

The title compound was prepared starting from 4-(piperazin-1-yl)quinazoline and 2-hydroxybenzaldehyde using the same procedure described for **3a** to afford white solid (50.4% yield): mp 118–120 °C; ^{1}H NMR ($CDCl_3$) δ 8.74 (s, 1H), 7.90 (dd, J = 0.66 Hz, J = 8.40 Hz, 1H), 7.84 (dd, J = 0.90 Hz, J = 8.46 Hz, 1H), 7.73 (ddd, J = 1.56 Hz, J = 7.08 Hz, J = 8.46 Hz, 1H), 7.45 (ddd, J = 1.20 Hz, J = 6.84 Hz, J = 8.22 Hz, 1H), 7.19 (td, J = 1.68 Hz, J = 8.04 Hz, 1H), 6.99 (dd, J = 1.38 Hz, J = 7.38 Hz, 1H), 6.85 (dd, J = 1.02 Hz, J = 8.04 Hz, 1H), 6.80 (td, J = 1.02 Hz, J = 7.38 Hz, 1H), 3.84 (s, 4H), 3.78 (s, 2H), 3.76 (s, 4H); ^{13}C NMR ($CDCl_3$) δ 164.6, 157.6, 154.1, 151.9, 132.7, 129.2, 128.9, 125.7, 124.8, 120.8, 119.5, 116.7, 116.3, 61.7, 52.5, 49.6; MS Calcd for $C_{19}H_{20}N_4O$ 320.1637. Found MS (DART-TOF) m/z 321.1730 $(M+H)^+$.

4.2.12. Synthesis of 4-(4-benzylpiperazin-1-yl)-2-phenylquinazoline (6a)

The title compound was prepared starting from2-phenyl-4-(piperazin-1-yl)quinazoline and benzaldehyde using the same procedure described for **3a** to afford white solid (40.2% yield): mp 118 °C; ^{1}H NMR ($CDCl_3$) δ 8.58–8.55 (m, 2H), 7.97 (dd, J = 0.72 Hz, J = 8.46 Hz, 1H), 7.88 (dd, J = 1.02 Hz, J = 8.46 Hz, 1H), 7.71 (ddd, J = 1.38 Hz, J = 6.90 Hz, J = 8.46 Hz, 1H), 7.51–7.45 (m, 3H), 7.41–7.33 (m,5H), 7.29 (tt, J = 1.56 Hz, J = 6.54 Hz, 1H), 3.89 (t, J = 4.68 Hz, 4H), 3.61 (s, 2H), 2.69 (t, J = 4.80 Hz, 4H); ^{13}C NMR ($CDCl_3$) δ 164.9, 159.5, 152.9, 132.4, 130.2, 129.3, 129.0, 128.5, 128.4, 127.3, 125.0, 124.9, 115.5, 63.2, 53.1, 49.9; MS Calcd for $C_{25}H_{24}N_4$ 380.2001. Found MS (DART-TOF) m/z 381.2075 $(M+H)^+$.

4.2.13. Synthesis of 4-(4-benzylpiperazin-1-yl)quinazoline (6b)

The title compound was prepared starting from 4-(piperazin-1-yl)quinazoline and benzaldehyde using the same procedure described for **3a** to afford pale yellow solid (35.1% yield): mp 100–102 °C; ^{1}H NMR ($CDCl_3$) δ 8.71 (s, 1H), 7.88 (dd, J = 0.54 Hz, J = 8.42 Hz, 1H), 7.87 (dd, J = 0.90 Hz, J = 8.52 Hz, 1H), 7.71 (ddd, J = 1.38 Hz, J = 7.02 Hz, 1H), 7.42 (ddd, J = 1.20 Hz, J = 7.08 Hz, J = 8.28 Hz, 1H), 7.37–7.31 (m, 4H), 7.27 (tt, J = 1.74 Hz, J = 6.84 Hz, 1H), 3.80 (t, J = 4.68 Hz, 4H), 3.59 (s, 2H), 3.65 (t, J = 4.80 Hz, 4H); ^{13}C NMR ($CDCl_3$) δ 164.6, 154.1, 151.8, 137.6, 132.5, 129.3, 128.6, 128.4, 128.3, 127.4, 125.4, 125.1, 63.1, 53.0, 49.8; MS Calcd for $C_{19}H_{20}N_4$ 304.1688. Found MS (DART-TOF) m/z 305.1777 $(M+H)^+$.

4.3. Molecular docking

Model building and binding energy calculation of designed compounds were carried out by Autodock 4.2 and the structural information was illustrated by Discovery Studio 3.1. In brief, the crystal structure of NF-κB & DNA complex (PDB code: 1LE5) was obtained from Protein Data Bank. The DNA molecule was removed and hydrogen atoms were added. One hundred different conformations of each designed molecule were generated by Lamarkian algorithm and docked to the putative drug binding region.[13] The lowest binding energy of each molecule conformer was calculated using the default parameters of Autodock 4.

4.4. Cell growth inhibition assay

Cells were plated in 96-well plates and allowed to adhere for 24 h and the T_0 plate was fixed and treated according to the SRB protocol. The compounds at appropriate concentration were added into the sample plates and incubate for 1 h at 37 °C followed by stimulation with 20 ng/ml TNF-α of some wells. The cells were then incubated for an additional 48 h before fixation. The plates were washed and air dried. Into each well was added 50 μl 0.4% w/v sulphorhodamine B (SRB) (Sigma–Aldrich) at room temperature for 30 minutes, followed by washing with 1% acetic acid. The bound stain was solubilized with 10 mM Tris base and the OD was read at 515 nm. One-way ANOVA was employed to detect significant differences between mean values.

4.5. Luciferase assay

HepG2 cells were cultured in Dulbecco's Modified Eagle Medium (DMEM) supplemented with 10% fetal bovine serum, 100 U/ml of penicillin and 100 μg/ml of streptomycin. The cells were plated in 96-well plates and transfected using the lipofectamine 2000 (Invitrogen) with 10 ng/well pGL 4.32 NF-κB-Luc (Promega) and Renilla control in Opti-MEM reduced serum medium (Invitrogen) following the protocol provided by manufacturers. Test compounds were dissolved in DMSO and added at the appropriate concentration to the 96-well plate with fresh medium and the plates were then incubated at 37 °C for 1 h. For induction of transcription, TNF-α was added (final concentration: 20 ng/ml) and the cells were incubated for an additional 6 h before lysis with passive lysis buffer. The luciferase and Renilla activity were measured in a 96-well plate using the Dual-Luciferase Reporter (DLR) Assay Systems (Promega). The luciferase activity was determined as the relative light units of firefly luciferase activity per unit of *Renilla reniformis* luciferase. One-way ANOVA was employed to detect significant differences beween mean values.

4.6. TUNEL assay

Terminal deoxynucleotidyltransferase (TdT) nick-end labeling (TUNEL) assay was performed on slides with a Trevigen TACS 2 TdT (TBL) kit (Trevigen) following the protocol provided by the manufacturer. In brief, EKVX cells were cultured RPMI 1640 with 10% fetal bovine serum, 100 U/ml of penicillin and 100 μg/ml of streptomycin and seeded on sterile glass coverslips placed in 12-well plates. The cells were treated with designed compound at the appropriate concentration for 1 h at 37 °C and then stimulated with 20 ng/ml TNF-α for another 18 h. After fixing the cells with 3.7% paraformaldehyde, the cells were covered with proteinase K solution for 30 min, followed by the treatment of labeling reaction mix, stop buffer, Strep_Fluorescein Solution and DAPI stain.

Acknowledgments

The authors appreciate funding from a Graduate Student Research Grant (LX) from UOP PCSP committee and Eberhardt Research Fellowship (WAR) from UOP FRC. NMR instrumentation was facilitated by National Science Foundation grant MRI-0722654. The authors thank Dr. William Chan, Dr. Andreas Franz, Patrick Batoon and Liang Zhao for technical help and useful discussion. The authors also appreciate Dr. Kathy M. Giacomini and Dr. Ligong Chen for their gracious support of LX during internship at UCSF.

Supplementary data

Supplementary data associated with this article can be found, in the online version, at http://dx.doi.org/10.1016/j.bmc.2012.10.051. These data include MOL files and InChiKeys of the most important compounds described in this article.

References and notes

1. Karin, M.; Yamamoto, Y.; Wang, Q. M. *Nat. Rev. Drug Disc.* **2004**, *3*, 17.
2. Karin, M.; Lin, A. *Nat. Immunol.* **2002**, *3*, 221.
3. Pommier, Y.; Sordet, O.; Antony, S.; Hayward, R. L.; Kohn, K. W. *Oncogene* **2004**, *23*, 2934.
4. Kieran, M.; Blank, V.; Logeat, F.; Vandekerckhove, J.; Lottspeich, F.; Le Bail, O.; Urban, M.; Kourilsky, P.; Baeuerle, P.; Israel, A. *Cell* **1990**, *1007*, 62.
5. Baeuerle, P.; Baltimore, D. *Genes Dev.* **1989**, *3*, 1689.
6. Van Antwerp, D. J.; Martin, S. J.; Kafri, T.; Green, D. R.; Verma, I. M. *Science* **1996**, *274*, 787.
7. Baeuerle, P.; Baltimore, D. *Science* **1988**, *242*, 540.
8. Yamamoto, Y.; Gaynor, R. B. *J. Clin. Invest.* **2001**, *107*, 135.
9. Kobayashi, Y.; Yoshimori, A.; Kino, K.; Miyazawa, H.; Tanuma, S.-i. *Bioorg. Med. Chem.* **2009**, *17*, 5293.
10. Pande, V.; Sharma, R. K.; Inoue, J.-I.; Otsuka, M.; Ramos, M. J. *J. Comput. Aided Mol. Des.* **2003**, *17*, 825.
11. Tobe, M.; Isobe, Y.; Tomizawa, H.; Nagasaki, T.; Takahashi, H.; Fukazawa, T.; Hayashi, H. *Bioorg. Med. Chem.* **2003**, *11*, 383.
12. Qian, L.; Shen, Y.; Chen, J.-C.; Wang, Y.-X.; Wu, X.-T.; Chen, T.-J.; Zheng, K.-C. *QSAR Comb. Sci.* **2008**, *27*, 984.
13. Tsai, K.-C.; Teng, L.-W.; Shao, Y.-M.; Chen, Y.-C.; Lee, Y.-C.; Li, M.; Hsiao, N.-W. *Bioorg. Med. Chem. Lett.* **2009**, *19*, 5665.
14. Van Horssen, R.; Ten Hagen, T. L. M.; Eggermont, A. M. M. *Oncologist* **2006**, *11*, 397.
15. Matsumoto, N.; Ariga, A.; To-e, S.; Nakamura, H.; Agata, N.; Hirano, S.-i.; Inoue, J.-i.; Umezawa, K. *Bioorg. Med. Chem. Lett.* **2000**, *10*, 865.
16. Obtained from Cayman Chemical Company, Ann Arbor, MI, USA.
17. Monga, M.; Sausville, E. A. *Leukemia* **2002**, *16*, 520.
18. Skehan, P.; Storeng, R.; Scudiero, D.; Monks, A.; McMahon, J.; Vistica, D.; Warren, J. T.; Bokesch, H.; Kenney, S.; Boyd, M. R. *J. Natl. Cancer Inst.* **1990**, *82*, 1107.